recycling

MDPI

Article

Selective Recycling of Steel Sandwich Polyisocyanurate (PIR) Foam Insulation Cladding

Diana Meza-Rojas, James Holliman, David Penney, Anthony R. Lewis and Peter J. Holliman *

Faculty of Science and Engineering, Swansea University, Swansea SA1 8EN, UK; d.penney@swansea.ac.uk (D.P.); anthony.r.lewis@swansea.ac.uk (A.R.L.)
* Correspondence: p.j.holliman@swansea.ac.uk

Abstract

A method has been developed to delaminate the organic components (paint, foam) from the steel skins of composite polyisocyanurate (PIR) steel insulation panels at ambient temperature and in 20 min using selected solvents combined with ultrasonication. Using this method, polyisocyanurate foam can be selectively delaminated from polymer-based paint (PVC plastisol) and, in turn, the polymer paint can be selectively delaminated from the galvanised steel. Both the foam and paint are removed as intact layers, leaving the galvanised steel intact for the next steps of recycling, enabling the subsequent individualised recycling of each sub-component or layer. Several solvents have been tested, and the data show that H-bonding solvents (e.g., H_2O, alcohols) are less effective at delaminating these polymers. Whilst high polarity, medium H-bonding acetonitrile and DMSO remove PVC paint and some PIR foam, the most effective solvent for both PIR foam and PVC paint removal is medium polarity, medium H-bonding acetone.

Keywords: delamination; organic coated steel; insulation foams; paint; infrared spectroscopy; corrosion inhibitor; circular economy

1. Introduction

In recent years, energy-related CO_2 emissions from buildings have increased despite the urgent need to reduce greenhouse gas emissions [1]. Current data indicates that one third of energy demand and 40% of direct/indirect CO_2 emissions are related to the construction and building sector. To meet climate targets (e.g., net zero domestic greenhouse gas emissions by 2050), [2] insulation panels can be applied to building envelopes to improve heat management. In this context, the current industry leading material used in building foam insulation panels are polyisocyanurate (PIR) foams, and panels of this type can achieve thermal conductivity values as low as 0.02 W/mK [3]. Whilst such panels are designed to last for 40 years in operation, this paper addresses the question of how to disassemble them at the end of building life.

To date, most reports have focussed on the recycling of the individual components of composite insulation panels, i.e., PIR foam, organic paints (polyurethane—PU, polyvinyl chloride—PVC) or galvanised steel. The difficulty in recycling PIR foams is reflected by Yang et al. who state that, whilst recycling should be the ideal option, landfill or incineration occur more frequently in reality [4]. Previous reports on methods to recycle PIR, polymer and paint include pyrolysis of PIR at 660 °C [5] which showed 55% of the material unaccounted for (lost as volatiles or within the transfer lines) with the other main products being less useful CO_2 (10.7%) and char (21.2%). The pyrolysis of rigid

Check for updates

Academic Editor: Denis Rodrigue

Received: 12 February 2026
Revised: 12 March 2026
Accepted: 23 March 2026
Published: 1 April 2026

Copyright: © 2026 by the authors. Licensee MDPI, Basel, Switzerland. This article is an open access article distributed under the terms and conditions of the Creative Commons Attribution (CC BY) license.

polyurethane has been studied between 250 and 460 °C to produce volatile fuels with Py-GC/MS identifying predominantly oxygen-containing alcohols, esters and ethers as volatile products [6]. The synergistic co-pyrolysis of polyurethane with paulownia wood has also been studied at 500 °C [7] suggesting that alkali metals in the wood catalyse PU pyrolysis whilst wood pyrolysis free radicals promote PU pyrolysed polyester polyols to cyclise. Behrendt and Naber have reviewed thermal and chemical PU recycling, concluding that PU recycling is complicated by the number of PU formulations manufactured even from a single site [8]. Glycolysis of PU and PIR has been reported using dipropylene glycol, a CH_3CO_2K catalyst 180–220 °C [9] and hydrolysis by NaOH in ethanol/water at 80 °C in 2 h producing polyol and a benzene derivative [10]. Stache et al. have reported the photothermal conversions using white light LEDs of polystyrene/carbon black composites to styrene monomers with up to 60% conversion in 5 min [11] or PVC into (1-chloroethyl) benzene [12]. Lui et al. showed that milling flexible PU through seven cycles could produce ca. 100 μm particles which could replace up to 15% of the polyol in new PU foams [13]. By comparison, steel recycling is well-established at commercial scale [14,15], including galvanised steel, particularly through the electric arc furnace (EAF) route. However, the high temperatures used in EAFs mean that ideally all organic matter is removed from scrap to reduce organic-derived emissions.

However, much less has been reported on methods to delaminate the component layers of insulation panels [16]. In fact, much more has been reported on how to prevent delamination to extend product lifetimes, including solar panels [17,18], woven structures [19], galvanised steel [20,21] and organic coated steel [22–24]. Whilst this is clearly important, the fact remains that full separation of the component parts is essential to disassemble the panels and avoid the cross-contamination of sub-components if they are all to be fully recycled. This also raises the generic recycling question of how you recycle a product which has been specifically designed for long-term operational deployment (i.e., 40 years for steel insulation panels). This paper addresses this question by reporting a method to selectively delaminate either paint and/or foam from composite steel insulation panels.

2. Results

Composite building insulation panels typically consist of an insulation core material (e.g., PIR foam) sandwiched between two painted steel skins (Figure 1). The architecture of Colorcoat HPS200 Ultra® layers is illustrated in [25].

The substantial differences in material properties and dimensions of the foam (e.g., ca. 20.00 cm width, density of ca. 60 kg/m^3, compressive strength ca. 190 kPa [26]) versus the steel skins (ca. 0.65 cm width and a density of ca. 7850 kg/m^3, compressive strength > 250 MPa) make it relatively straightforward to separate the majority of the PIR foam from the steel. This leaves the steel skins with residual foam on the surface (the area highlighted with the red dashed box in Figure 1).

Whilst this sandwich arrangement appears simple, in practice, the architecture is more complex because the steel skins have a surface layer of zinc as a galvanic protection against corrosion (Figure 2). Then, the outermost surfaces of both the inner and outer facing zinc layers are both coated with primer layers. The primer layer which faces the outside of the building is then coated with a polymer-based paint. In this paper, this is labelled the "paint side". The primer layer which faces the inside of the building is coated with PIR foam. In this paper, this is labelled the "foam side". Figure 2a shows this layer-by-layer arrangement schematically showing that there are six interfaces across one side of the composite panel rather than just a simple foam–metal interface. All of these interfaces must be delaminated from each other to fully recycle all the panel sub-components.

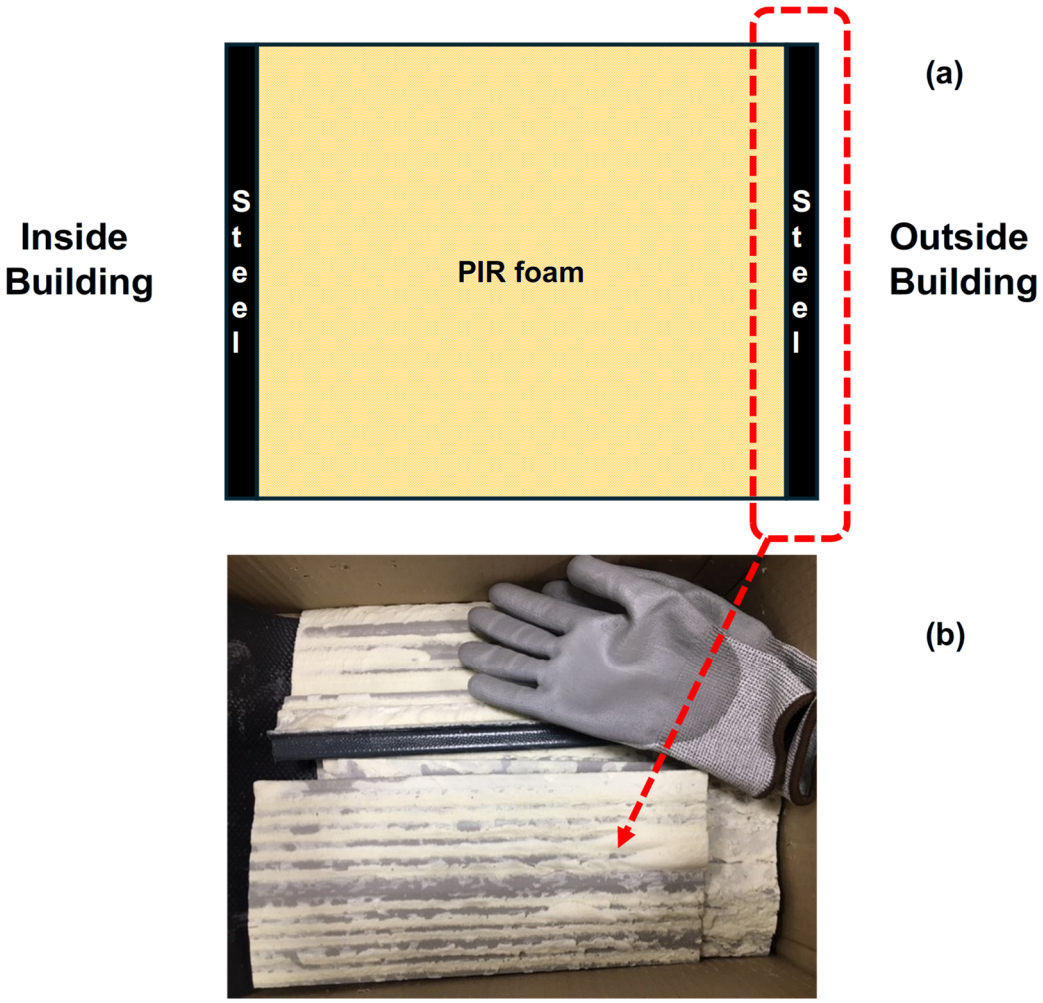

Figure 1. (**a**) Schematic of PIR foam–steel sandwich cladding panels and (**b**) sections of commercial panels (ca. 30 × 15 cm) with the majority of PIR foam mechanically removed. The red dotted line indicates where one steel skin has been removed and used for delamination testing with examples of the resulting samples shown in (**b**).

Figure 2 also shows the different layer thicknesses in the panel stack. Looking at the paint side first, the zinc galvanic layer is ca. 25 µm thick, followed by the primer layer (ca. 7–8 µm thick) and the PVC plastisol paint layer (ca. 200–300 µm thick). Comparing this with the foam side, the zinc galvanic layer is very similar at ca. 15 µm thick, but the primer is slightly thicker at ca. 8–9 µm thick and the residual PIR foam layer is thicker again at ca. 1800 µm thick. These layer thicknesses need to be put into the context of commercial insulation panel sizes which are typically 1 m wide and several metres long. These factors generate several barriers to recycling these insulation panels which need to be overcome. So, the very high aspect ratio of individual layers to panel size makes mechanical recycling processes less efficient because the layers will separate at the weakest point. Here, this removes most of the PIR foam from the metal strip but leaves a residual layer of ca. 2 mm of PIR foam on the metal. After this, the strong adhesion of the remaining layers to their underlying substrate layer combined with the fact that they are thin films relative to the size of the panels makes removing any other layers using mechanical processing very difficult. However, the residual paint and foam need to be separated from the steel strip so the metal can be re-melted and recycled in an Electric Arc Furnace (EAF) without contamination from any organic material which might otherwise generate volatile organic

matter in the emissions. Ideally, the recycled organic materials need to be recovered without compromising their physico-chemical properties [27].

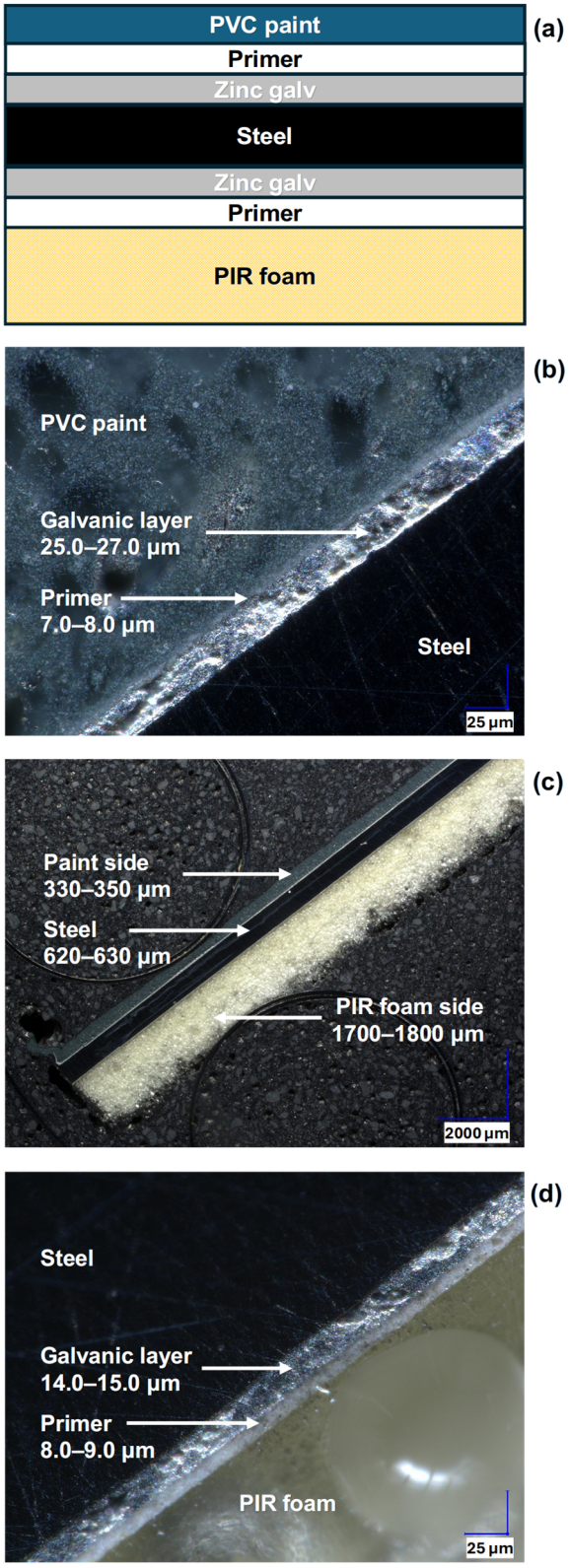

Figure 2. Cross-sectional microscopy of galvanised steel composite panel showing (**a**) sub-component layered architecture, (**b**) detail of paint–galvanic layer interface—scale bar = 25 µm, (**c**) overview of paint–metal–foam region—scale bar = 2000 µm and (**d**) detail of foam–galvanic layer interface—scale bar = 25 µm.

This suggests some kind of low temperature chemically based process is required. As such, we have studied the use of solvents in parallel with sonication. Sonication has been reported previously as a method to exfoliate two-dimensional materials [28] where the aspect ratio would be expected to be high.

Table 1 shows data from the visual analysis of composite panel samples which have either been soaked overnight in solvent or sonicated for 20 min with both treatments at room temperature (images for all the treatments are shown in the ESI). Looking at the sonication treatment, the data show that alcohol-based solvents (i.e., methanol, ethanol or propanol) all behave in a similar manner in that they remove the majority, but not all, of the foam layer. However, they are ineffective at removing the paint layer. A similar pattern of behaviour is observed for these solvents after 24 h of soaking except that propanol removes neither paint nor foam under these conditions.

Table 1. Visual analysis data for layer removal using solvents and methods shown.

Solvent	Method	Paint Layer Coverage (% Area)		Foam Layer Coverage (% Area)	
		Before	After	Before	After
Methanol	Sonicate, 20 min	100	100	95	5
	24 h soak	100	100	84	11
Ethanol	Sonicate, 20 min	100	100	91	19
	24 h soak	100	100	99	7
Propanol	Sonicate, 20 min	100	100	82	15
	24 h soak	100	100	97	97
Acetone	Sonicate, 20 min	100	0	87	4
	24 h soak	100	0	99	0
Acetone/H_2O 50:50 *v*/*v*	Sonicate, 20 min	100	70	99	18
Acetonitrile	Sonicate, 20 min	100	0	98	2
DMSO	Sonicate, 20 min	100	0	99	4
$NaOH_{(aq)}$	Sonicate, 20 min	100	100	99	83
	24 h soak	100	100	100	100

The most successful solvents at removing the PIR foam and the PVC plastisol paint layer are acetone (see for example Figure 3) and acetonitrile. On visual inspection, both these solvents appear to remove either all or the vast majority of the organic material from the metal substrate. Interestingly, dimethyl sulphoxide (DMSO) behaves in the opposite manner to the alcohol-based solvents because it is effective at removing the paint layer and most of the PIR foam, whilst methanol only removes the PIR foam and does not delaminate the paint. These data are interesting because they indicate that selective delamination of either the paint or the PIR foam may be possible using different solvents. Similar results are also observed when the samples are soaked for 24 h in the solvent without sonication.

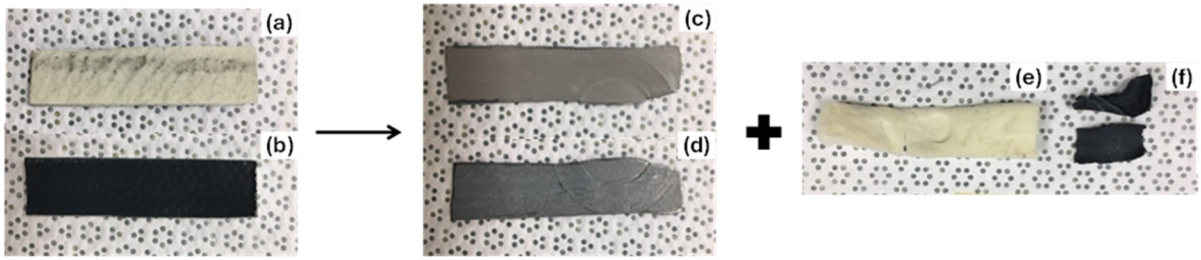

Figure 3. Sample (ca. 10 × 40 mm) before treatment showing (**a**) foam side and (**b**) paint side, then after sonication for 20 min in acetone showing (**c**) foam side, (**d**) paint side, (**e**) delaminated PIR foam and (**f**) delaminated paint.

The water-based solvents (e.g., aqueous sodium hydroxide or the 50:50 acetone/water mix) are not as effective as the organic solvents. This is unsurprising given that these products have been designed and optimised to extend their operational lifetime for external use under typical weathering exposure. Given that operational guarantees of up to 40 years are possible (depending on typical weather conditions), the delamination resistance to rain ingress of these products is a key performance feature. Again, similar data are observed when the samples are soaked for 24 h in the solvent without sonication, with no delamination for $NaOH_{(aq)}$ and partial delamination for acetone/water.

In this paper, we report the delamination of PIR foam and PVC paint coatings from galvanised steel. Although we are not attempting total dissolution of the polymer layers, some consideration of polymer solubility is helpful to explain the effects of the various solvents used. Two possibilities here are the Flory–Huggins or Hansen solubility parameters [29]. However, it has been reported that experimental measurements of the Flory–Huggins parameter are time consuming and require expensive equipment [29] so here we have considered Hansen parameters instead (Table 2) [30,31]. The data show that the solvents have similar dispersion (or van der Waals) parameters but that they can be grouped into four based on their polarity and hydrogen bonding as follows: water has high polarity and very high H-bonding, ethanol and methanol have medium polarity and high H-bonding, acetonitrile and DMSO have high polarity and medium H-bonding and acetone has medium polarity and H-bonding. Correlating this with the delamination data (Table 1), there is no foam or paint removal for aqueous NaOH and only paint removal for methanol and ethanol. This shows that hydrogen bonding is less helpful for delaminating PIR foam. In turn, for the lower H-bonding solvents, the higher polarity of acetonitrile and DMSO is less helpful for PIR removal with only partial delamination. The most effective delamination solvent for both PIR foam and PVC paint is the medium polarity/H-bonding acetone, suggesting that the foam has similar characteristics.

Table 2. Hansen solubility parameters [30,31] for selected solvents where δ_d = dispersion, δ_p = dipole–dipole and δ_h = hydrogen bonding parameters, respectively.

Solvent	δ_d	δ_p	δ_h
Acetone	15.5	10.4	7.0
Methanol	15.1	12.3	22.3
Ethanol	15.8	8.8	19.4
Acetonitrile	15.3	18.0	6.1
DMSO	18.4	16.4	10.2
Water	15.6	16.0	42.3

The resultant materials have been analysed using infrared spectroscopy (Figure 4). Looking first at the metal substrate on the foam side after the PIR foam has been removed (Figure 4a), there are characteristic peaks for residual PIR remaining on the surface. For example, there is a broad peak at 3350 cm^{-1} corresponding to an N-H stretch mode, three medium intensity peaks in the range 2800–3000 cm^{-1} for C-H stretching modes and thre characteristically intense peaks for polyisocyanurate at ca. 1730 cm^{-1} for a C=O stretching mode, 1530 cm^{-1} for an N-H bending mode and 1410 cm^{-1} for a C-N stretching mode associated with the cyanurate ring [32]. However, there is a clear absence of the intense PIR-related peaks observed for the foam side of the metal substrate. By comparison, the ATR-IR spectrum of the metal substrate on the paint side after the PVC plastisol paint has been removed (Figure 4a), shows fewer peaks in the 600–4000 cm^{-1} region which is consistent with susbstantial paint (organic matter) removal. For example, there is a very weak, broad peak around 3400 cm^{-1} for an O-H stretching mode associated with residual surface moisture. There are also peaks present which are consistent with residual

polyvinyl chloride polymer. For example, the three peaks between 2800 and 3000 cm^{-1} are C-H stretching modes and the less intense C=O stretch ca. 1730 cm^{-1} is for residual plasticiser [33]. The weaker peaks at 1250 and 1330 cm^{-1} are for characteristic Cl-C-H skeletal vibration of the PVC structure [12,34].

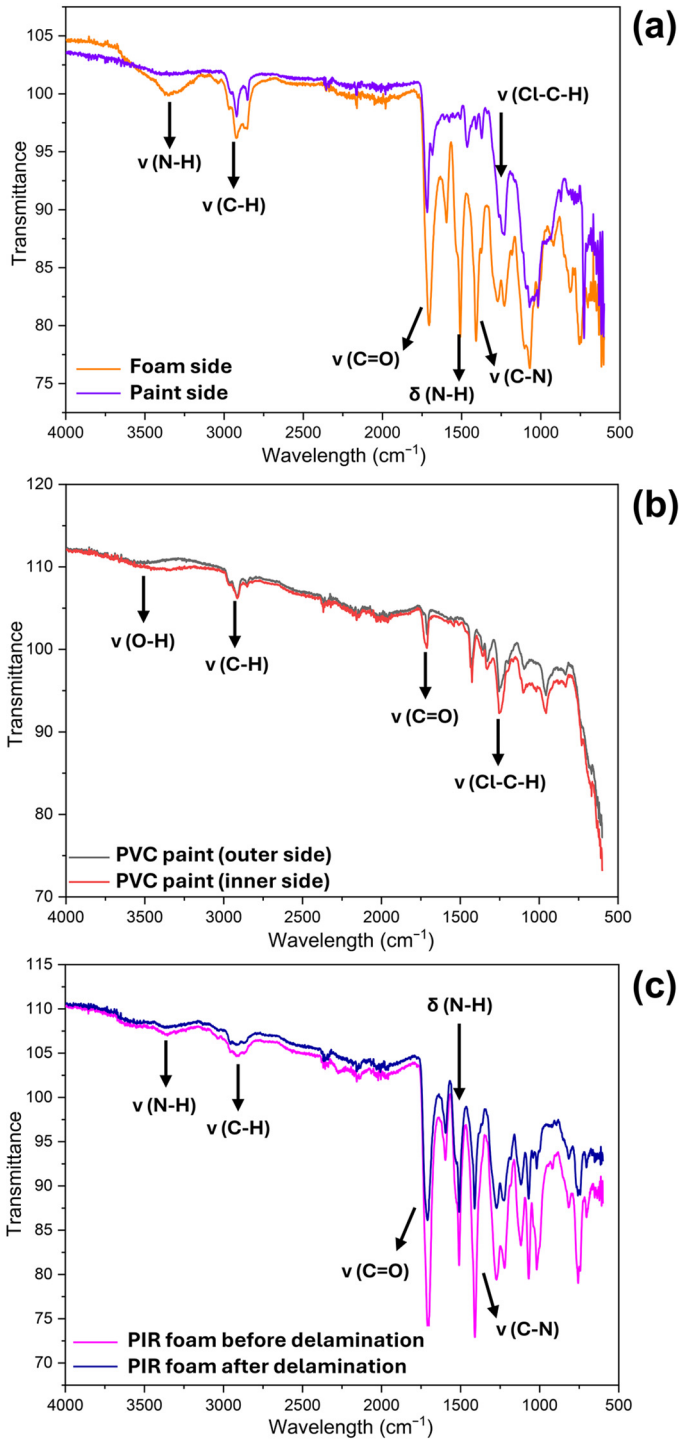

Figure 4. Attenuated total reflectance-infrared (ATR-IR) spectra of (**a**) metal substrate surfaces after delamination, (**b**) delaminated PVC plastisol paint and (**c**) PIR foam before and after delamination.

Figure 4b shows the ATR-IR data for both the outer and inner sides of the delaminated PVC plastisol paint. Not surprisingly, these two spectra are very similar to each other and to the spectrum of the paint side of the metal substrate which suggests that the paint film has not been chemically damaged during the delamination process. At first sight, the

intensity of the delaminated paint film peaks appears less intense than the metal substrate (Figure 4a paint side) which might infer less PVC is present which is not in line with the delaminated sample which is just PVC plastisol film. This is due to the increase in the background absorption at <750 cm^{-1} which is ascribed to the presence of pigments in the black paint film which have been removed from the metal surface.

Figure 4c shows the ATR-IR data for the PIR foam before and after delamination. Here again, the two spectra are very similar, suggesting that very little chemical change occurs to the PIR foam during delamination. There is also no evidence for residual acetone held within the PIR matrix. This is not surprising because all the evidence suggests the solvent front diffuses through the polymer to the interface to induce delamination. This can be seen to occur passively overnight or in 20 min when sonicated. Once the polymer is removed from the bulk solvent, it seems logical that the solvent should diffuse to the edges of the foam and evaporate. Similar effects are observed in other polymers. For example, solvents (including acetone) are used to enhance the electrical conductivity of PEDOT:PSS (poly(3,4-ethylenedioxythiophene): polystyrene sulphonate) films [35,36], but it is known that these solvents diffuse out of these films, and this can be studied by the loss of electrical conductivity over time [37].

3. Discussion

Looking at a potential delamination mechanism based on these results (Table 1, Figures 3 and 4), the data clearly show that sonicating the samples in organic solvent increases the rate of reaction. It is important to note that these are thin polymer films adhered to metal substrates. Hence, if we consider the aspect ratio of these samples, the thickest layer is the foam which is ca. 2 mm thick compared to a 10 × 40 mm sample size. At face value, this is an aspect ratio of between 5:1 and 20:1. However, the situation is more complex because these PIR foams consist of closed cells (ca. 100–200 μm in size) of PIR polymer where the cell walls are typically 9–12 μm thick (Figure 5f). Hence, a 2 mm thick PIR foam represents a depth of approximately 10–20 cells between the solvent and the primer-foam interface. This is a PIR polymer thickness of between 90 μm (10 cells with 9 μm thick walls) and 240 μm (20 cells with 12 μm thick walls). So, in practice, the microporosity of the PIR foam changes the aspect ratio to between 40:1 and 440:1. By comparison, the aspect ratio is simpler to calculate for the PVC plastisol paint because it does not contain microporous cells. It is between 12:1 and 50:1 for the ca. 200 μm thick PVC plastisol paint.

This aspect ratio is important when considering the rate of diffusion of organic solvent to the polymer–primer interface where delamination occurs. The aspect ratio data combined with the successful delamination in 20 min suggest rapid rates of mass transport. This suggests diffusion occurs through the polymer layers rather than by ingress at the cut edges of the samples. The solvent diffusion will stop when the solvent front reaches the organic–primer interface. Solvent-induced polymer swelling (which is a ubiquitous phenomenon (e.g., [38–40]) then induces tension at the polymer–primer interface. The adhesion here results from the high aspect ratio such that the polymer layer adheres to the primer through the collective action of huge numbers of van der Waals interactions. Although each individual van der Waals interaction is weak, their collective bond strength produces a strongly adhered layer. However, the solvent-induced polymer swelling can disrupt the van der Waals interactions across the entire surface which causes the delamination of the polymer from the primer-coated metal. The substantial increase in the rate of delamination (from 20 min by sonication versus 24 h by passive soaking) suggests that increases the rate of solvent diffusion through the polymer films resulting from the sonication causing localised vibrations within the polymer structure.

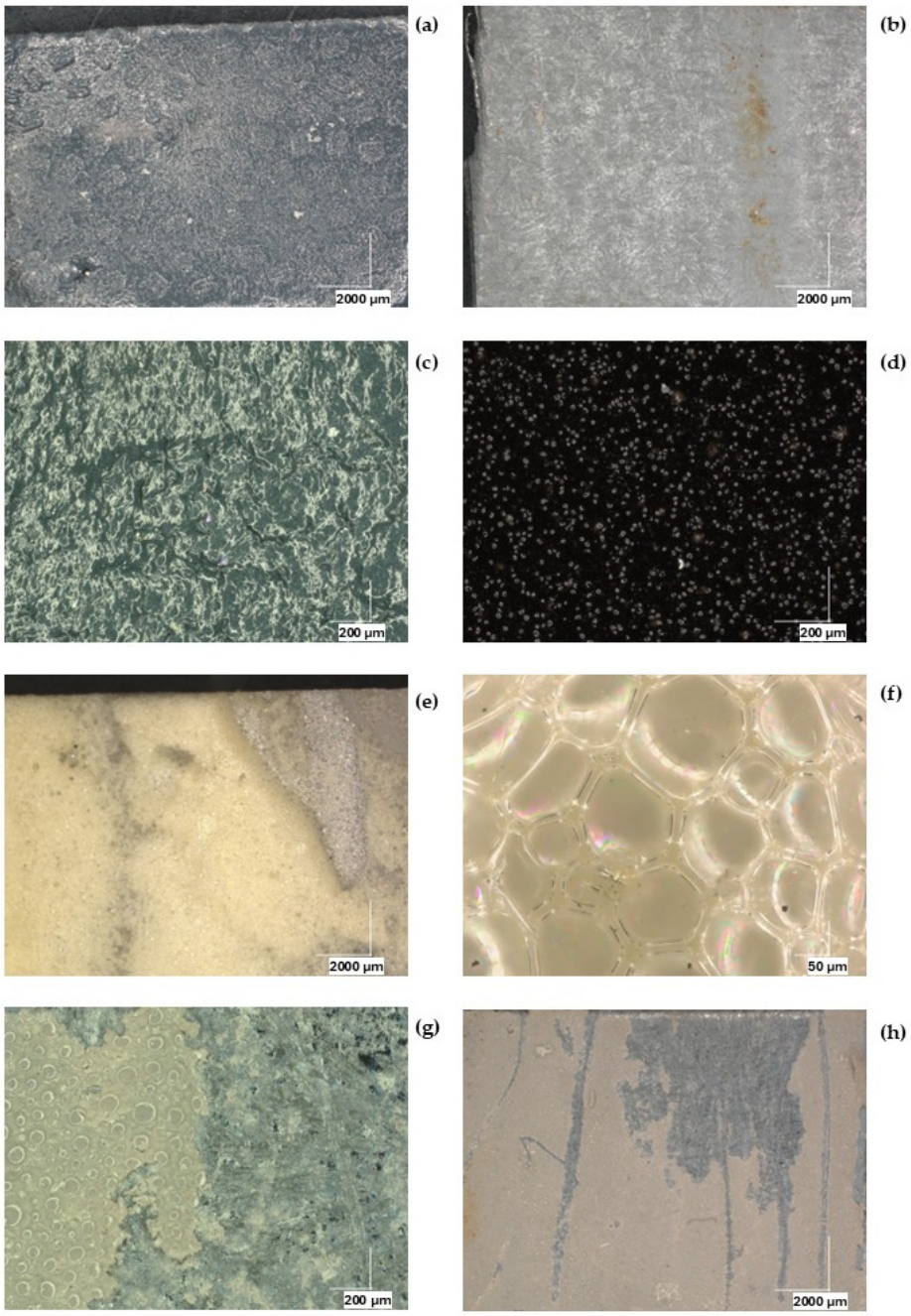

Figure 5. Optical micrographs of (**a**) underside of delaminated PVC plastisol paint layer (**b**) exposed galvanised steel surface after PVC plastisol paint delamination, (**c**) close-up of delaminated PVC plastisol paint layer, (**d**) external surface of delaminated PVC plastisol paint, (**e**) PIR foam attached to steel skin before delamination, (**f**) close-up of PIR foam showing closed cell structure and cell walls, (**g**) exposed galvanised steel after PIR delamination and (**h**) partially delaminated polyester primer layer and exposed galvanised steel.

When considering delamination mechanisms, looking at the PVC plastisol paint layer first, Figure 5a shows an embossed pattern on the underside of the delaminated paint which is the inverse of the surface roughness pattern on the corresponding, exposed galvanised steel surface. Figure 5c shows a close-up of the adhesive surface of the delaminated PVC plastisol paint with a high degree of surface topography, suggesting physical rather than chemical adhesion dominates at the PVC paint–galvanic layer interface. The data also show a clean removal of the PVC plastisol paint whilst Figure 5d shows the outermost layer of the PVC plastisol paint is unchanged relative to the untreated, adhered PVC plastisol paint.

Looking at the PIR foam layer, Figure 5e,f show the sample from the foam side before delamination. Figure 5e shows different thicknesses of the PIR foam in line with the shearing of the bulk of the foam from the steel skin while Figure 5f shows the closed cells of the PIR and the single wall thickness (10–15 μm) between those cells. Figure 5g shows the interface between the PIR foam and the galvanised steel after delamination. The data show a thin film of residual PIR which has not foamed during manufacturing but rather forms the adhesive layer to the zinc. The shadow of cells can be seen but they are separated from each other (ca. 100 μm) apart. Hence, the data suggest that the foam delaminates by the breaking of the walls of the first set of PIR cells above the zinc-PIR interface. Finally, Figure 5h confirms that the extremely thin polyester primer layer is only partially removed. The polyester primer layer remains largely adhered to the galvanised steel after delamination of the PIR foam and PVC plastisol paint. This is advantageous from a recycling perspective, as the primer layer is extremely thin and does not compromise downstream electric arc furnace steel recycling. Moreover, retention of the primer suggests that delamination occurs preferentially at the organic polymer–prime interface rather than at the zinc–steel interface, preserving the integrity of the galvanised substrate.

4. Materials and Methods

Composite insulation panels from Building Systems UK Ltd. (Shotton, UK) —a Tata Steel Enterprise consisting of an insulating PIR core between 2 metal facings (Figure 1a) first had most of the foam core removed by shear force. This left residual foam on top of a primer layer adhered to galvanised steel (Figure 1b). The foam/paint/galvanised steel panels were then cut into smaller coupons (ca. 1 × 4 cm) ready for the recycling experiments.

For recycling, the foam/paint/galvanised steel coupons were placed in a Pyrex beaker (Merck Life Science UK Ltd., Dorset, UK) with selected solvent (e.g., acetone, methanol, ethanol, 2-propanol, acetonitrile, dimethyl sulfoxide or a 50:50 *v*:*v* acetone/water mix). All solvent treatments were performed on at least three independent samples, with consistent delamination behaviour observed across replicates. The solvents were chosen to provide a range of polarity and polymer-solvent interaction strengths (from alcohols to aprotic polar solvents), allowing systematic evaluation of solvent diffusion and swelling effects on PIR foam and PVC plastisol paint delamination. The samples were then placed into a water-filled ultrasound bath and sonicated for 20 min at room temperature. The coupons were then removed from the solvent and an initial visual analysis carried out to identify any delamination of the components.

Further analysis of the extent of delamination was carried by loading the digital images into ImageJ 1.54g. The images were then converted to 32-bit greyscale and using the default model a threshold value was applied to mask the area where foam or paint was still located. The area fraction or organic layer was then calculated.

Further analysis of the surfaces of the sub-component products was carried out using attenuated total reflectance-infrared spectroscopy (ATR-IR) using a Perkin Elmer Attenuated Total Reflectance-Infrared Spectrometer (ATR-IR Spectrum Two) (PerkinElmer (UK) Ltd., High Wycombe, UK).

For cross-sectional image analysis, samples were suspended in resin. Once the resin had cured, the samples were lightly sanded and polished using diamond slurry to a 1 μm finish and imaged using optical and scanning electron microscopy (OM and SEM, respectively). OM was carried out using a Keyence VHX-7000 (Keyence, Birmingham, UK) at magnifications ranging from 20 to 1000 times. SEM was measured on a Hitachi TM3000 Scanning Electron Microscope (SEM) (Hitachi High-Tech Europe GmbH, Krefeld, Germany)

with Bruker Energy Dispersive X-ray Spectroscopy (EDS) module (Bruker Nano GmbH, Berlin, Germany).

5. Conclusions

Composite steel insulation panels are specifically engineered for long-term durability, which presents significant challenges for end-of-life recycling. This paper presents what we believe to be the first example of a method to selectively delaminate multi-layer composite stacks which are made up of a polyisocyanurate foam which is adhered to organic polymer (PVC plastisol) paint which is adhered to a galvanised steel substrate. The data show that a solvent-based sonication process can delaminate the different organic components (i.e., PIR foam and paint) of the insulated steel panel individually into intact materials to enable them to be fully recycled. The process can be carried out passively overnight or more rapidly (20 min) by sonication. In both cases, delamination takes place at ambient temperature which prevents thermal damage to the polymers. The process is simple, requiring only the correct solvent choice and sonication which should help its scalability. The recycling method also produces clean, galvanised steel which is no longer contaminated by foam or paint and so is compatible with electric arc furnace (EAF) steel recycling because it will add no unwanted carbon emissions.

Author Contributions: Conceptualization, D.M.-R., J.H. and P.J.H.; methodology, D.M.-R., J.H. and P.J.H.; validation, P.J.H. and D.P.; formal analysis, D.M.-R., J.H., P.J.H., D.P. and A.R.L.; investigation, D.M.-R. and J.H.; data curation, D.M.-R., J.H., P.J.H., D.P. and A.R.L.; writing—original draft preparation, D.M.-R., J.H. and P.J.H.; writing—review and editing, J.H., P.J.H. and D.P.; supervision, P.J.H. and D.P.; project administration, P.J.H. and D.P.; funding acquisition, P.J.H. All authors have read and agreed to the published version of the manuscript.

Funding: This research was funded by Swansea University's EPSRC Impact Acceleration Account 2022–2026 for supporting DMR, grant number EP/X525637/1; EPSRC for funding the Sustain Hub for PJH and AL, grant number EP/S018107/1; and Building Systems UK—a Tata Steel Enterprise and EPSRC for co-sponsoring an iCASE PhD for JH, grant number EP/Y528638/1.

Data Availability Statement: The original contributions presented in this study are included in the article. Further inquiries can be directed to the corresponding author.

Acknowledgments: We gratefully thank Julia Lloyd, Jonathan Arnold (Building Systems UK Ltd.—a Tata Steel Enterprise) and Kevin Tinkham (Tata Steel Colors R&D) for supply of samples and helpful discussions.

Conflicts of Interest: The authors declare no conflicts of interest.

References

1. Available online: https://www.iea.org/energy-system/buildings (accessed on 17 January 2026).
2. UK Govt. *Climate Change Strategy*; Ministry of Justice, UK Government: London, UK, 2021. Available online: https://www.gov.uk/government/publications/climate-change-and-sustainability-strategy-moj/climate-change-and-sustainability-strategy (accessed on 17 January 2026).
3. Gravit, M.; Kuleshin, A.; Khametgalieva, E.; Karakozova, I. Technical characteristics of rigid sprayed PUR and PIR foams used in construction industry. *IOP Conf. Ser. Earth Environ. Sci.* **2017**, *90*, 012187. [CrossRef]
4. Yang, W.; Dong, Q.; Liu, S.; Xie, H.; Liu, L.; Li, J. Recycling and disposal methods for polyurethane foam wastes. *Procedia Environ. Sci.* **2012**, *16*, 167–175. [CrossRef]
5. Eschenbacher, A.; Varghese, R.J.; Weng, J.; Van Geem, K.M. Fast pyrolysis of polyurethanes and polyisocyanurate with and without flame retardant: Compounds of interest for chemical recycling. *J. Anal. Appl. Pyrolysis* **2021**, *160*, 105374. [CrossRef]
6. Jiang, L.; Zhang, D.; Li, M.; He, J.-J.; Gao, Z.-H.; Zhou, Y.; Sun, J.-H. Pyrolytic behavior of waste extruded polystyrene and rigid polyurethane by multi kinetics methods and Py-GC/MS. *Fuel* **2018**, *222*, 11–20. [CrossRef]
7. Li, K.; Xu, Y.; Ye, Z.; Huang, X.; Wu, X.; Zou, Y. Co-pyrolysis of thermoplastic polyurethane with paulownia wood: Synergistic effects on product properties and kinetics. *Fuel* **2024**, *361*, 130623. [CrossRef]

8. Behrendt, G.; Naber, B.W. The Chemical Recycling of Polyurethanes (Review). *J. Univ. Chem. Technol. Metall.* **2009**, *44*, 3–23.
9. Modesti, M.; Costantini, F.; dal Lago, E.; Piovesan, F.; Roso, M.; Boaretti, C.; Lorenzetti, A. Valuable secondary raw material by chemical recycling of polyisocyanurate foams. *Polym. Degrad. Stab.* **2018**, *156*, 151–160. [CrossRef]
10. Liu, L.-J.; Wang, X.-L.; Gu, Z.-Y.; Ren, X.-L.; Chang, T. Rapid hydrolysis of waste polyurethane and facile system separation. *Sep. Purif. Technol.* **2025**, *354*, 129068. [CrossRef]
11. Oh, S.; Jiang, H.; Kugelmass, L.H.; Stache, E.E. Recycling of Post-Consumer Waste Polystyrene Using Commercial Plastic Additives. *ACS Cent. Sci.* **2025**, *11*, 57–65. [CrossRef]
12. Jiang, H.; Medina, E.A.; Stache, E.F. Upcycling Poly (vinyl chloride) and Polystyrene Plastics Using Photothermal Conversion. *J. Am. Chem. Soc.* **2025**, *147*, 2822–2828. [CrossRef] [PubMed]
13. Guo, L.; Wang, W.; Guo, X.; Hao, K.; Liu, H.; Xu, Y.; Liu, G.; Guo, S.; Bai, L.; Ren, D.; et al. Recycling of Flexible Polyurethane Foams by Regrinding Scraps into Powder to Replace Polyol for Re-Foaming. *Materials* **2022**, *15*, 6047. [CrossRef]
14. Danny Harvey, L.D. Iron and steel recycling: Review, conceptual model, irreducible mining requirements, and energy implications. *Renew. Sustain. Energy Rev.* **2021**, *138*, 110553. [CrossRef]
15. Davis, C.; Li, Z.; Styring, P.; Curry, R.; Holliman, P.J. Routes to reducing emissions from steel production. *Nat. Rev. Clean Technol.* **2025**, *1*, 890–902. [CrossRef]
16. Djemai, H.; Labed, A.; Hecini, M.; Djoudi, T. Delamination analysis of composite sandwich plate of cork agglomerate/glass fiber-polyester: An experimental investigation. *Rev. Compos. Matériaux Avancés-J. Compos. Adv. Mater.* **2021**, *31*, 193–197. [CrossRef]
17. Hasan, A.A.Q.; Ahmed Alkahtani, A.; Shahahmadi, S.A.; Nur, E.; Alam, M.; Islam, M.A.; Amin, N. Delamination-and Electromigration-Related Failures in Solar Panels—A Review. *Sustainability* **2021**, *13*, 6882. [CrossRef]
18. Murillo, A.; Buceta, A.; Urbina, A.; Jaione Bengoechea, J. Impact of melting range on delamination process and recycling potential of photovoltaic encapsulants. *Sol. Energy Mater. Sol. Cells* **2026**, *294*, 113884. [CrossRef]
19. Vorhof, M.; Sennewald, C.; Schegner, P.; Pham, M.Q.; Hoffmann, G.; Gereke, T.; Cherif, C. Lightweight panels with high delamination resistance made of integrally woven truss-like fabric structures. *J. Ind. Text.* **2023**, *53*, 15280837221150202. [CrossRef]
20. Hausbrand, R.; Stratmann, M.; Rohwerder, M. Corrosion of zinc–magnesium coatings: Mechanism of paint delamination. *Corros. Sci.* **2009**, *51*, 2107–2114. [CrossRef]
21. Phelps, L.L. Investigation of Coating Delamination Failure from Factory-Primed Galvanized Decking. In Proceedings of the AMPP Conference 2025, Nashville, TN, USA, 6–10 April 2025; pp. 1–10. [CrossRef]
22. Holness, R.J.; Williams, G.; Worsley, D.A.; McMurray, H.N. Polyaniline Inhibition of Corrosion-Driven Organic Coating Cathodic Delamination on Iron. *J. Electrochem. Soc.* **2005**, *152*, B73. [CrossRef]
23. Klimow, G.; Fink, N.; Grundmeier, G. Electrochemical studies of the inhibition of the cathodic delamination of organically coated galvanised steel by thin conversion films. *Electrochim. Acta* **2007**, *53*, 1290–1299. [CrossRef]
24. Glover, C.F.; Williams, G. Inhibition of corrosion-driven organic coating delamination and filiform corrosion on iron by phenyl phosphonic acid. *Prog. Org. Coat.* **2017**, *102*, 44–52. [CrossRef]
25. Tata Steel UK Limited. *Colorcoat HPS200 Ultra Technical*; Tata Steel UK Limited: London, UK, 2024.
26. Lazo, M.; Puga, I.; Macías, M.A.; Barragán, A.; Manzano, P.; Rivas, A.; Rigail-Cedeño, A. Mechanical and thermal properties of polyisocyanurate rigid foams reinforced with agricultural waste. *Case Stud. Chem. Environ. Eng.* **2023**, *8*, 100392. [CrossRef]
27. Hummen, T.; Sudheshwar, A. Fitness of product and service design for closed-loop material recycling: A framework and indicator. *Resour. Conserv. Recycl.* **2023**, *190*, 106661. [CrossRef]
28. Contreras-Pereda, N.; Hayati, P.; Suárez-García, S.; Esrafili, L.; Retailleau, P.; Benmansour, S.; Novio, F.; Morsali, A.; Ruiz-Molina, D. Delamination of 2D coordination polymers: The role of solvent and ultrasound. *Ultrason. Sonochemistry* **2019**, *55*, 186–195. [CrossRef] [PubMed]
29. Ethier, J.; Antoniu, E.R.; Brettmann, B. Predicting polymer solubility from phase diagrams to compatibility: A perspective on challenges and opportunities. *Soft Matter* **2024**, *20*, 5652–5669. [CrossRef] [PubMed]
30. Subrahmanyam, R.; Gurikov, P.; Dieringer, P.; Sun, M.; Irina Smirnova, I. On the Road to Biopolymer Aerogels—Dealing with the Solvent. *Gels* **2015**, *1*, 291–313. [CrossRef]
31. Trivedi, H.K.; Yadav, R.K.; Meshram, A.; Gupta, R. Removal of encapsulant ethylene-vinyl acetate for recycling of photovoltaic modules: Hansen solubility parameters analysis. *Process Saf. Environ. Prot.* **2024**, *186*, 1397–1409. [CrossRef]
32. Reignier, J.; Méchin, F.; Sarbu, A. Chemical gradients in PIR foams as probed by ATR-FTIR analysis and consequences on fire resistance. *Polym. Test.* **2021**, *93*, 106972. [CrossRef]
33. Rybachuk, G.V.; Kozlova, I.I.; Mozzhukhin, V.B.; Guzeev, V.V. PVC Plastisols: Preparation, Properties, and Application. *Polym. Sci. Ser. C* **2007**, *49*, 6–12. [CrossRef]
34. Mallakpoura, S.; Shafiee, E. The synthesis of poly (vinyl chloride) nanocomposite films containing ZrO_2 nanoparticles modified with vitamin B1 with the aim of improving the mechanical, thermal and optical properties. *Des. Monomers Polym.* **2017**, *20*, 378–388. [CrossRef]

35. Yousefian, H.; Babaei-Ghazvini, A.; Akbar Isari, A.; Hashemi, S.A.; Acharya, B.; Ghaffarkhah, A.; Arjmand, M. Solvent-doped PEDOT:PSS: Structural transformations towards enhanced electrical conductivity and transferable electromagnetic shields. *Surf. Interfaces* **2024**, *51*, 104481. [CrossRef]
36. McQuade, J.; Vuong, L.T. Solvent Retention and Crack Evolution in Dropcast PEDOT:PSS and Dependence on Surface Wetting. *ACS Omega* **2018**, *3*, 3868–3873. [CrossRef] [PubMed]
37. Alshammari, A.S. Effect of solvents treatment on the electrical stability and surface wetting properties of PEDOT:PSS thin films. *Mater. Lett.* **2019**, *250*, 30–33. [CrossRef]
38. Zhu, M.; Vesely, D. The effect of polymer swelling and resistance to flow on solvent diffusion and permeability. *Eur. Polym. J.* **2007**, *43*, 4503–4515. [CrossRef]
39. Mukherji, D.; Marques, C.M.; Stuehn, T.; Kremer, K. Depleted depletion drives polymer swelling in poor solvent mixtures. *Nat. Commun.* **2017**, *8*, 1374. [CrossRef]
40. Bajd, F.; Mikac, U.; Mohorič, A.; Serša, I. The Effect of Polymer–Solvent Interaction on the Swelling of Polymer Matrix Tablets: A Magnetic Resonance Microscopy Study Complemented by Bond Fluctuation Model Simulations. *Polymers* **2024**, *16*, 601. [CrossRef]

Disclaimer/Publisher's Note: The statements, opinions and data contained in all publications are solely those of the individual author(s) and contributor(s) and not of MDPI and/or the editor(s). MDPI and/or the editor(s) disclaim responsibility for any injury to people or property resulting from any ideas, methods, instructions or products referred to in the content.